# Nanoparticle-Mediated Cytoplasmic Delivery of Proteins To Target Cellular Machinery

**Shyam Sundhar Bale, Seok Joon Kwon, Dhiral A. Shah, Akhilesh Banerjee, Jonathan S. Dordick,* and Ravi S. Kane***

Department of Chemical and Biological Engineering, Rensselaer Polytechnic Institute, Troy, New York 12180

ARTICLE

**ABSTRACT** Despite recent advances in nanomaterial-based delivery systems, their applicability as carriers of cargo, especially proteins for targeting cellular components and manipulating cell function, is not well-understood. Herein, we demonstrate the ability of hydrophobic silica nanoparticles to deliver proteins, including enzymes and antibodies, to a diverse set of mammalian cells, including human cancer cells and rat stem cells, while preserving the activity of the biomolecule post-delivery. Specifically, we have explored the delivery and cytosolic activity of hydrophobically functionalized silica nanoparticle−protein conjugates in a human breast cancer cell line (MCF-7) and rat neural stem cells (NSCs) and elucidated the mechanism of cytosolic transport. Importantly, the proteins were delivered to the cytosol without extended entrapment in the endosomes, which facilitated the retention of biological activity of the delivered proteins. As a result, delivery of ribonuclease A (RNase A) and the antibody to phospho-Akt (pAkt) resulted in the initiation of cell death. Delivery of control protein conjugates (*e.g.*, those containing green fluorescent protein or goat antirabbit IgG) resulted in minimal cell death, indicating that the carrier-mediated toxicity was low. The results presented here provide insight into the design of nanomaterials as protein carriers that enable control of cell function.

**KEYWORDS:** protein delivery · nanoparticle−protein conjugates · mechanism of cellular uptake · signaling pathways · stem cell delivery

The introduction of specific proteins into cells represents a powerful alternative to methods of manipulating cellular function based on the introduction of genetic material, which is the current standard method for expression of specific proteins in cells.[1,2] For example, unlike loss of function screens that typically involve cellular transfection with constructs that express shRNA, protein delivery to the cell can be used to assess loss/gain of function on different post-translationally modified forms of a protein, for example, on various kinases involved in cellular signaling.[3−5] In addition, it may be advantageous to deliver certain complex proteins (*e.g.*, multicomponent protein assemblies or post-translationally modified proteins) to cells because these proteins may require exquisite cellular machinery for their production, which may not be present or fully functional in the host cell. By introducing proteins that specifically recognize and influence target proteins, deactivation or activation of key signaling pathways within the cell can occur, which will strongly affect cell function.[6]

A variety of carriers have been studied for their applicability as delivery agents, including (but not limited to) liposomes, polymeric micelles, and nanomaterials.[7−14] Liposomes are phospholipid vesicles of varying diameters, which can be loaded with biomolecules and are considered ideal materials for drug delivery due to their biological inertness and biocompatibility. However, the efficiency of liposomal delivery of proteins is generally low and depends on cell type; for example, only 30−80% of cells actually receive the protein of interest.[15,16] Recent studies have shown the ability of nanoscale materials to act as carriers to transport biomolecular cargo into mammalian cells.[10,11,13] While a variety of nanoscale carriers, including quantum dots, nanoparticles, and carbon nanotubes, have been shown to be internalized by cells, the mechanism of internalization remains unclear. For instance, while some reports indicate a non-endocytotic mechanism of uptake, several other studies suggest a key role for endocytosis.[11,12,17−20] Furthermore, the presence of biomolecular cargo can interfere with nanomaterial−membrane interactions and influence the mechanism and efficiency of internalization. Moreover, most of the delivered biomolecules may get entrapped in vesicular compartments, such as endosomes, rendering them ineffective for targeting cellular components.[12,21] As a result, two critical criteria for efficient protein delivery to mammalian cells are not met: (a) efficient delivery of proteins to the cell

*Address correspondence to dordick@rpi.edu, kaner@rpi.edu.

Received for review November 10, 2009 and accepted February 23, 2010.

**Published online March 4, 2010.**
**10.1021/nn901586e**

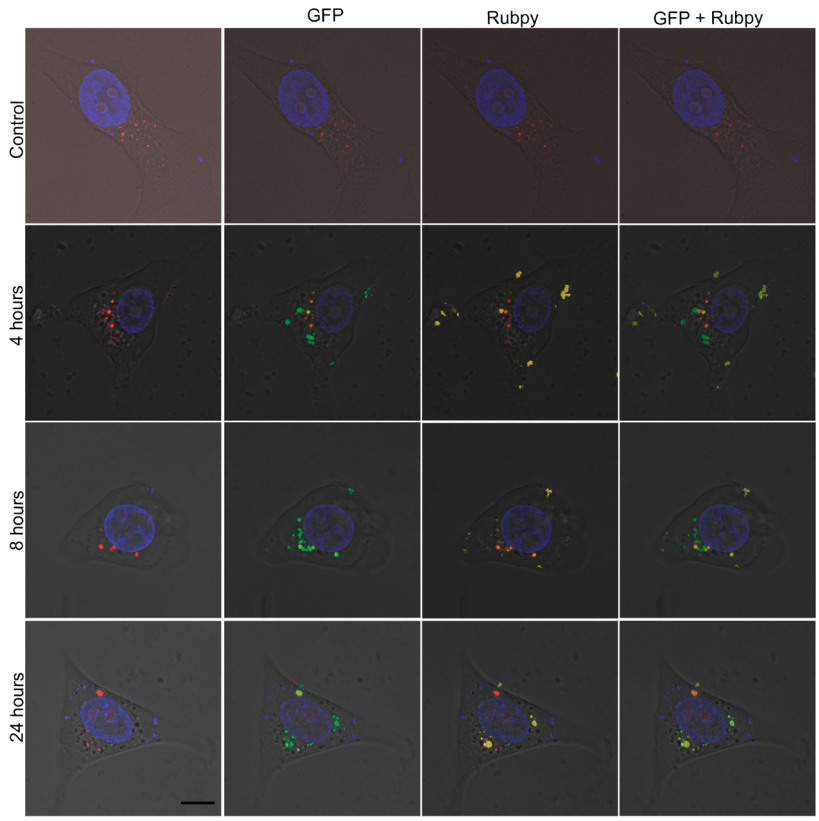


**Figure 1. Characterization of the internalization of Rubpy-doped SiNP−ODMS−GFP conjugates by confocal microscopy. Multilabel cell images showing the internalization of nanoparticles at varying time periods of incubation. The nucleus was stained using DAPI (blue), and the lysosomal compartments were stained using lysotracker (red). Images are from *z*-stacks and were obtained at thickness intervals of 1 μm. Scale bar represents 10 μm.**

cytoplasm, and (b) retention of biological activity at the targeted site of action.

Herein, we explore the ability of hydrophobic silica nanoparticles to immobilize and effectively deliver proteins to the cytoplasm of mammalian cells while enabling retention of biological activity of the delivered protein. Specifically, we have delivered functionalized silica nanoparticle−protein conjugates to a human breast cancer cell line (MCF-7) and to rat neural stem cells (NSCs). In the process, the mechanism of autonomous escape of these nanoparticle−protein conjugates from the endosomal compartments has been elucidated. Finally, by delivering specific proteins, we were able to control cell fate by manipulating the cellular machinery and signaling pathways.

## RESULTS AND DISCUSSION

Confocal laser scanning microscopy and epifluorescence microscopy were used to characterize the delivery of nanoparticle−protein conjugates to the cytoplasm of target cells. For initial experiments, green fluorescent protein (GFP)[22] was used as a model protein; in addition to serving as a reagentless marker that can be used to assess retention of protein structure and function, GFP also serves as a simple reporter to follow nanoparticle−protein conjugate delivery into cells. Initial experiments were carried out using conjugates of dye (Rubpy)-doped silica nanoparticles as the nanoscale vehicle, which allowed us to track simultaneously the intracellular location of both the nanoparticle and the protein. The silica nanoparticles (20 nm) were functionalized with *n*-octadecyltrimethoxysilane (*n*-ODMS); these functionalized nanoparticles will henceforth be referred to as SiNPs. Conjugate formation was carried out *via* simple adsorption (see Materials and Methods). Immobilized GFP retained *ca.* 60−70% of its fluorescence, which indicates the favorable retention of structure after immobilization onto the nanomaterial.

MCF-7 cells were used as the initial mammalian host, and 0.1 mg/mL of Rubpy−SiNP−GFP conjugates were incubated with the cells for 24 h. Following lysosomal and nuclear staining, confocal microscopy was used to characterize the internalization of the Rubpy−SiNP−GFP conjugates (Figure 1). Every image in Figure 1 also includes the nuclear (DAPI, blue) and lysosomal (lysotracker, red) stains. As seen in Figure 1, the SiNP−GFP conjugates were internalized in less than 4 h, and conjugates were clearly observed in the cell cytosol (up to 24 h) and outside the endosomal compartments (Movies M1−4 and Figure S1 in Supporting Information). Throughout the process, GFP retained its fluorescence, which indicates that the delivery process was not harsh and did not deactivate the conjugated protein. Furthermore, colocalization of the fluorescence signals from the Rubpy−SiNP and GFP (Figure 1 and Figure S1) provides evidence of the integrity and stability of the conjugates after delivery to the cytosol.

Fluorescence activated cell sorting (FACS) analysis confirmed cellular delivery. Specifically, MCF-7 cells were incubated with increasing concentrations (up to 0.4 mg/mL) of SiNP−GFP conjugates for 14 h (Figure 2a). Analysis of ~5000 cells revealed a clear shift in fluorescence intensity in the FITC channel, consistent with GFP entry into the cells. Delivery of the nonfluorescent SiNP−BSA conjugates as a control did not result in change in the fluorescence intensity of cells (Figure 2b). The near complete shift in the histogram of Figure 2a indicates that essentially all of the cells internalized the SiNP−GFP conjugates. In contrast, a significantly smaller increase in the fluorescence intensity was observed using a liposomal protein delivery system (ProJect, Pierce), and very little change in fluorescent intensity was observed using GFP alone (Figure 2c).

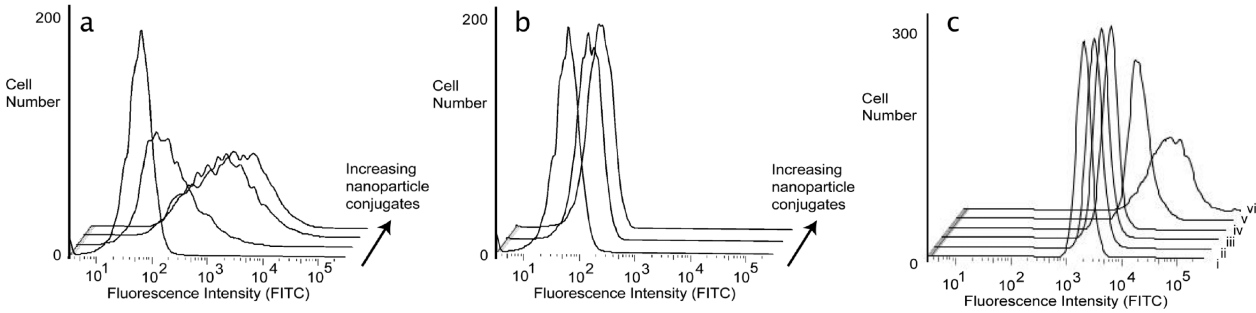


**Figure 2. FACS analysis of internalization of SiNP−protein conjugates. Data are recorded on the FITC channel ($\lambda_{ex}$ = 488 nm, $\lambda_{em}$ = 515 nm). (a) Flow cytometry histograms showing the internalization of SiNP−GFP conjugates after an overnight incubation (14 h). Histograms showing the fluorescence profile of cells incubated with 0, 0.05, 0.2, and 0.4 mg/mL of nanoparticle−protein conjugates (30 μg GFP immobilized per 1 mg SiNP). (b) Delivery of SiNP−BSA to MCF-7 cells; flow cytometry histograms showing no increase in fluorescence signal for cells incubated overnight (14 h) with SiNP−BSA conjugates. (c) Comparison of GFP delivery with various carriers; flow cytometry histograms showing the fluorescence profile of (i) cells and of cells incubated with (ii) GFP (2.5 μg), (iii) GFP (40 μg), (iv) Pro-Ject (2.5 μg of GFP), (v) Pro-Ject (40 μg of GFP), and (vi) 0.1 mg/mL (2.5 μg of immobilized GFP) of nanoparticle−protein conjugates.**

Collectively, the confocal microscopy and FACS results indicate efficient nanoparticle-mediated delivery of GFP to the cytosol of host cells.

Having established the efficient delivery of SiNP−GFP to MCF-7 cells, we proceeded to assess whether the delivery mediated by these hydrophobic nanoparticles would be toxic. To that end, we incubated MCF-7 cells with different concentrations of SiNP−GFP conjugates for 14 h followed by measurements of cell viability with the Trypan Blue reagent (Figure 3). Cell viability was *ca.* 84% at concentrations of the conjugates as high as 0.8 mg/mL, indicating the absence of significant nanoparticle-derived toxicity for these nanoparticle−protein conjugates. When coupled with the observation that essentially all cells internalized SiNP−GFP (Figure 2a), this information indicates that SiNP−protein conjugates have minimal toxicity.

Understanding the mechanism of internalization is critical for the efficient use of nanoparticles to deliver active proteins to the cytoplasm. A common route for nanoparticle delivery to mammalian cells involves endocytosis followed by release into the cytosol. However, several competing mechanisms may contribute to uptake. These could include phagocytosis, clathrin- and caveola-dependent endocytotic mechanisms, and involvement of other cellular machinery.[23] Our initial results (Figures 1 and 2) are consistent with the endocytotic uptake of SiNP−protein conjugates followed by autonomous release from the vesicular compartments that are involved in uptake. To further elucidate the mechanism(s) of internalization, we immobilized fluorescein−bovine serum albumin (FITC−BSA) on SiNPs and characterized their uptake by MCF-7 cells in the presence or absence of a variety of inhibitors for known endocytotic mechanisms. The fluorescence signal from FITC−BSA is *ca.* 10-fold higher when compared to that from GFP, which increases the sensitivity of FACS measurements (Supporting Information Figure S2).

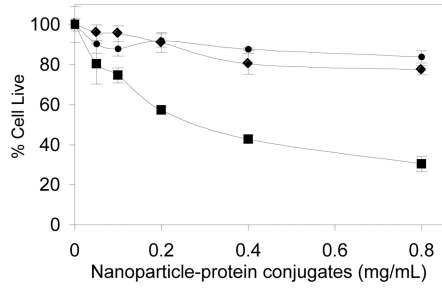


**Figure 3. Influence of nanoparticle−protein conjugates on the viability of mammalian cells. MCF-7 cells were exposed to increasing concentrations of SiNP−GFP (●), SiNP−RNase A (■), or SiNP-denaturated−RNase A (◆) conjugates for 14 h. Cell viability was then determined using the Trypan Blue assay.**

To elucidate the mechanism of cellular delivery of SiNP, we studied the effect of inhibitors of various endocytotic mechanisms, including phenylarsine oxide (PAO, 3 μM; clathrin inhibitor), cytochalasin D (Cyt D, 3 μM; actin inhibitor), filipin (Fili, 3 μg/mL; caveola inhibitor).[20] We also characterized the uptake of the conjugates at 4 °C with and without sodium azide ($NaN_3$, 0.05%).[13] Sodium azide inhibits energy-dependent endocytotic processes.[24,25] Cells were incubated with 0.1 mg/mL of SiNP−FITC−BSA conjugates and FACS analysis (Figure 4a) was used to characterize the uptake of the conjugates. Strong inhibition of nanoparticle uptake (*ca.* 55−65%) was indicated by the decrease in FITC signal (average from FACS analysis) in the presence of PAO and Cyt D. Furthermore, experiments at 4 °C in the presence of 0.05% $NaN_3$ showed a similar decrease in the FITC signal, supporting the involvement of energy-dependent endocytotic mechanisms in the uptake of the conjugates by MCF-7 cells. Confocal microscopy images of cells incubated with nanoparticle−protein conjugates in the presence of endocytotic inhibitors (Figure 4b−e) show uptake of conjugates, suggesting a possible role for other cellular machinery, as well. Collectively, these results suggest the strong involvement of clathrin-coated pits and actin microfilaments in the active uptake of SiNP−protein conjugates by MCF-7 cells.

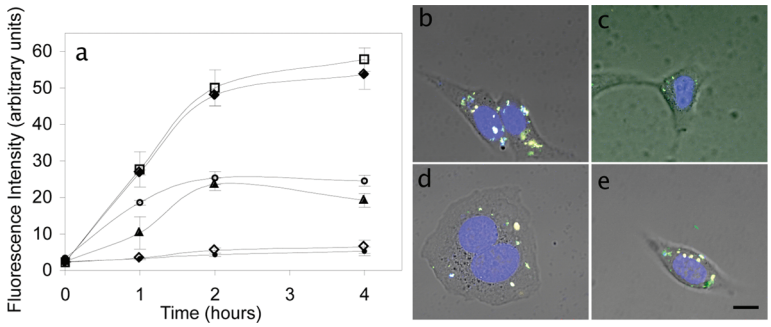


**Figure 4. (a) FACS analysis illustrating the role of endocytosis in the uptake of SiNP−FITC−BSA conjugates. Plot showing the increase in mean fluorescence values with time for cells incubated with nanoparticle−protein conjugates at 37 °C (◆), at 37 °C in the presence of filipin (□), cytochalasin D (▲), phenylarsine oxide (○), 4 °C (●) and at 4 °C with 0.05% sodium azide (◇). Confocal micrograph figures showing cells incubated with SiNP−FITC−BSA conjugates with (b) no inhibitor, (c) Cyt D (3 μM), (d) PAO (3 μM), (e) Fili (3 μg/mL). Scale bar represents 10 μm.**

To validate internalization and to demonstrate retention of biological function of the SiNP−protein conjugates, we used proteins that could disrupt cell function only upon entry into the cytosol. Among the multitude of ways cell function can be altered, we focused on two approaches: cytotoxicity due to degradation of critical cellular machinery and cytotoxicity due to disruption of key signaling pathways. With respect to the former, one protein that could strongly influence cell function is ribonuclease A (RNase A), which would have deleterious effects on cell viability by degrading mRNA and tRNA, thus inhibiting protein synthesis.[26] A dose response toxicity profile of SiNP−RNase A conjugates (a maximum exposure of 35 μg/mL of immobilized RNase A at 0.8 mg/mL nanoparticle addition) revealed statistically significant dose-dependent cytotoxicity that was well above the basal cytotoxicity due to the SiNP (Figure 3). Furthermore, control incubations with conjugates of SiNP with heat-denatured RNase A showed no enhancement in cytotoxicity over that of SiNP−GFP. Finally, incubation of MCF-7 cells with the endosomal disruption agent, chloroquine, had minimal impact in enhancing the cytotoxic effect of RNase A; less than 15% enhancement of RNase-driven cytotoxicity was seen in the presence of chloroquine (Supporting Information Figure S3). In aggregate, these results suggest that SiNP−RNase A conjugates are endocytosed into the cell and rapidly exocytose into the cytosol where RNase A activity results in cell death.

In terms of the ability to disrupt key signaling pathways in the cell, we employed the monoclonal antibody to phospho-Akt (pAkt) as the protein conjugated to SiNP; pAkt plays a major role in epidermal growth factor receptor signal transduction pathways, leading to activation of nuclear factor-κB (NF-κB) and its nuclear translocation, and subsequent transcriptional activation of proteins involved in cell growth.[4] Blocking this pathway (*i.e.*, by preventing pAkt from performing its signaling role) results in degradation of NF-κB and activation of caspases, which activate apoptosis signaling leading to cell death (Figure 5a). We reasoned, therefore, that cytosolic delivery of the antibody to pAkt would inactivate pAkt, thereby activating a variety of suppressed pathways, including apoptosis by activation of caspases (Figure 5b). Similar to that obtained with SiNP−RNase A, dose-dependent cytotoxicity was observed with SiNP−anti-pAkt (a maximum exposure of 1 μg/mL of immobilized anti-pAkt antibody at 0.8 mg/mL nanoparticle addition) (Figure 5c); once again, this scenario can only occur if the protein was delivered to the cytosol. Furthermore, when cells were incubated with SiNP−anti-rabbit IgG (*e.g.*, a nonbinding, control mAb), no enhancement in cytotoxicity was observed over that of SiNP alone.

To further test the downstream effects of inactivating pAkt, we examined poly(ADP-ribose) polymerase (PARP) cleavage (Figure 5c, inset). In the absence of pAkt, the cytosolic caspase pathway is activated, which leads to PARP cleavage (Figure 5a). This apoptotic signal can be seen as the cleavage of PARP (116 kDa), into 89 and 24 kDa fragments.[27,28] Consistent with the cytotoxicity results, PARP cleavage was only observed following cytosolic delivery of the SiNP−anti-pAkt. These results clearly demonstrate the ability of SiNP−protein conjugates to enter the cytosol at concentrations sufficient to impact cell function.

Having demonstrated the ability of SiNP−protein conjugates to be delivered into the cytosol and influence cell function, we wanted to assess whether such delivery was somehow unique to transformed cell lines. Indeed, it is well-known that cancer cells are "leaky" and thus may be more amenable to SiNP−protein conjugate transport through the cell into the cytosol. Moreover, cancer cells have signaling pathway alterations, which are often the core event in transformation.[29] For this reason, we examined the generality of our approach by using stem cells. In addition to the unique properties of self-renewal and differentiation, stem cells are capable of dividing into a multitude of cell types.[30] Altering stem cell signaling, therefore, may be a way to impart control over stem cell growth and differentiation.[31] Importantly, stem cells are known to possess membrane integrity similar to that of normal cells. For these reasons, we performed a series of experiments directed toward the delivery of SiNP−protein conjugates to rat hippocampal neural stem cells (NSCs).[32]

We initially examined whether the SiNP−protein conjugates resulted in general cytotoxicity in the NSCs. As with MCF-7 cells, we performed a dose response study using SiNP−GFP. After 14 h incubation, little loss in cell viability occurred (Supporting Information Figure S4). To elucidate the mechanism of internalization and delivery of active proteins to the stem cell cytoplasm,

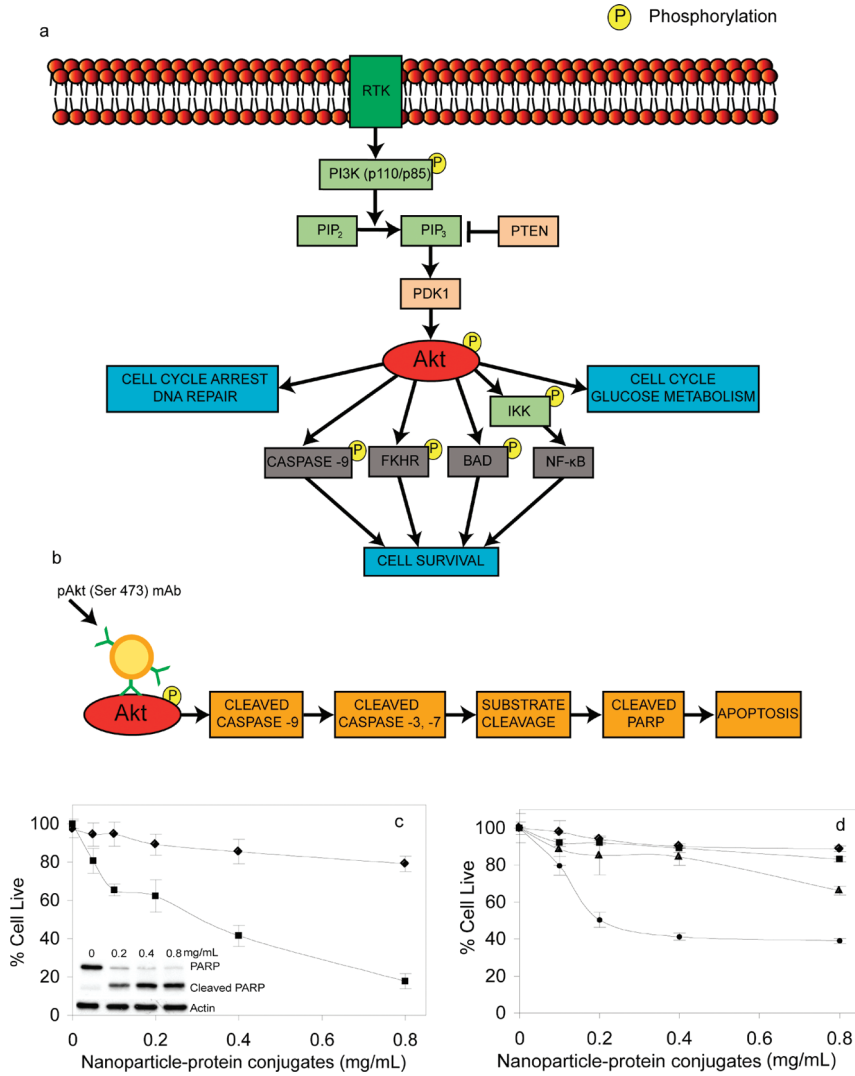


**Figure 5. Strategy for targeting metabolic pathways in cells. (a) Schematic of the Akt pathway. Activation of receptor tyrosine kinases (RTK) phosphorylates phosphoinositide 3-kinase (PI3K) in the cell cytoplasm. Akt is phosphorylated downstream of PI3K by a cascade involving phosphatidylinositol-3,4-diphosphate ($PIP_2$), phosphatidylinositol-3,4,5-triphosphate ($PIP_3$), and 3′-phosphoinositide-dependent kinase 1 (PDK1). Phosphorylated form of Akt has multiple targets and is involved in a variety of functions, including cell cycle arrest, DNA repair, glucose metabolism, and cell survival. Phospho-Akt phosphorylates caspase-9, forkhead (FKHR), BAD, and IkB kinase (IKK) and aids in cell survival. NF-κB, nuclear factor-κB; PTEN, phosphatase and tensin homologue. (b) Delivery of anti-phospho-Akt antibody initiates a cascade of downstream processes, including cleavage of PARP and apoptosis. (c) Influence of the delivery of nanoparticle−antibody conjugates on the viability of mammalian cells. MCF-7 cells were incubated with increasing concentrations of SiNP−anti-phospho-Akt (■) or control SiNP−antirabbit IgG (◆) conjugates for 14 h, and their viability was determined using the Trypan Blue assay. (Inset,c) Downstream effect of antibody delivery to mammalian cells. MCF-7 cells were exposed to increasing amounts of SiNP−anti-phospho-Akt conjugates for 14 h. Western blot analysis was then used to quantify the cleavage of PARP, a nuclear polymerase involved in DNA repair, and actin, which served as a control protein. Blocking phosphorylated Akt in the cell by the delivery of anti-phospho-Akt antibodies triggers activation of caspases. Activation of caspases leads to apoptosis, resulting in the cleavage of PARP. (d) Influence of delivery of nanoparticle−antibody conjugates on viability of stem cells. NSCs were incubated with increasing concentrations of SiNP−antirabbit IgG (◆, ■) and SiNP−anti-pAkt (▲,●) conjugates for 14 and 24 h, respectively, and their viability was determined using the Trypan Blue assay.**

we characterized the uptake of SiNP−FITC−BSA conjugates by NSCs in the presence or absence of a variety of inhibitors for known endocytotic mechanisms (as described above for MCF-7 cells). Specifically, NSCs were incubated with 0.1 mg/mL of SiNP−FITC−BSA conjugates, and FACS analysis (Figure S5) was used to characterize the uptake of the conjugates. Our results suggest a very strong inhibition of nanoparticle uptake in the presence of PAO and cytochalasin D, similar to that observed with MCF-7 cells. Furthermore, experiments at 4 °C in the presence of 0.05% $NaN_3$ support the involvement of energy-dependent endocytotic mechanisms in the uptake of the conjugates by NSCs. FACS data comparison with MCF-7 cells reveals a similar uptake by both the cell types, suggesting that it may be possible to use SiNPs to deliver proteins to many cell types. Toxicity assays indicated that the delivery of the anti-pAkt antibody caused stem cell death in a dose-

dependent manner (Figure 5d), however, at a longer incubation time than when compared with MCF-7 cells, presumably owing to the difference in the metabolic state of these cell lines. The cell viability decreased further upon 24 h incubation, suggesting a very efficient uptake of the conjugates and retention of activity of the immobilized antibody in the cell cytoplasm.

## CONCLUSION

Collectively, these results suggest the involvement of clathrin-coated pits and actin microfilaments in the active uptake of SiNP−protein conjugates by the different cell lines investigated, which include cancer (MCF-7) and stem (NSC) cells. The ability of nanoscale materials to autonomously escape from endosomal compartments can be used to deliver cargo that can alter cell metabolism and function and regulate signaling pathways. Such a system could have a broad applicability to target cellular function at a range of levels, including at the transcriptional, translational, and post-translational levels. This result has significant implications in understanding and applying the properties of nanoscale materials to not only stabilize biomolecules but also retain their activity post-delivery and could aid in the development of novel strategies for delivering biomolecule-based therapeutics.

## MATERIALS AND METHODS

**Cell Culture.** Human breast cancer (MCF-7) cells (American Type Cell Culture Collection) were maintained in Dulbecco's modified eagle's medium (DMEM) supplemented with 5% (v/v) fetal bovine serum (FBS) and 1% (v/v) penicillin/streptomycin mixture. Cell cultures were maintained at 37 °C and in 5% $CO_2$.

Adult rat neural stem cells (NSCs) isolated from the hippocampi of 6 week old female Fisher 344 rats were maintained in DMEM/F-12 medium supplemented with 1% (v/v) N2 supplement and 1% (v/v) penicillin/streptomycin mixture. Cell cultures were maintained in media with 20 ng/mL of fibroblast growth factor (FGF-2, Promega) in polyornithine/laminin (5 μg/mL, Sigma-Aldrich) coated plates at 37 °C and in 5% $CO_2$. Cells were subcultured at 70% confluency using Accutase (Phoenix Flow Systems, San Diego, CA). All materials were purchased from Invitrogen, Inc., unless stated.

**Functionalization of Nanoparticles.** Silica nanoparticles were first functionalized with *n*-octadecyltrimethoxysilane (*n*-ODMS). Silica nanoparticles (diameter = 15 ± 5 nm) were obtained from EKA Chemicals, Inc. (Augusta, GA), and Rubpy-doped silica nanoparticles (diameter = 15 ± 5 nm, $\lambda_{ex}$ = 458 nm, $\lambda_{em}$ = 592 nm) were obtained from Life Sciences Inc. Briefly, *ca.* 8 mg of silica nanoparticles was taken in 1 mL of dry ethanol and washed at least three times by centrifugation at 10 000 rpm for 5 min followed by redispersion in dry ethanol by sonication. Washed nanoparticles were then sonicated in a solution of 1% (v/v) *n*-ODMS in dry ethanol for 2 h. *n*-ODMS-functionalized silica nanoparticles were washed with dry ethanol three times followed by three washes with sterile PBS by repeated centrifugation and sonication as described above.

To attach proteins, *n*-ODMS-functionalized nanoparticles were suspended in sterile phosphate buffered saline (PBS) and a solution of protein in PBS was added to a final protein concentration of 1 mg/mL. The nanoparticle suspension was shaken at 200 rpm for 2 h at 4 °C. The resulting nanoparticle−protein conjugates were washed three times in PBS by repeated centrifugation at 7000 rpm for 5 min and redispersion by pipetting. Supernatants from all of the washes were collected, and the protein content was analyzed using the bicinchoninic acid (BCA) assay (Pierce Biotechnology, Rockford, IL). SiNP−protein conjugates were used immediately or stored at 4 °C. Values of the loading for GFP and RNase A were 30 ± 5 μg/mg SiNP and 40 ± 5 μg/mg SiNP, respectively. For conjugates of SiNP with anti-pAkt antibody, a mixture of 1.25 μg of antibody and 1.25 μg of BSA was loaded per milligram of SiNP.

**Confocal Microscopy.** Glass-bottom Petri dishes (35 mm total diameter, 22 mm glass bottom, Electron Microscopy Sciences, Hatfield, PA) were coated with poly-L-ornithine (0.01 mg/mL in sterile PBS) by overnight incubation and stored at −20 °C. Poly-L-ornithine-coated Petri dishes were washed with sterile PBS at least three times before using. MCF-7 cells in suspension were counted and diluted to 1 × $10^5$ cells/mL and seeded in poly-L-ornithine-coated Petri dishes at 1 × $10^5$ cells/dish. Cells were allowed to settle for 15 min, and 1 mL of fresh media was further added to the plate and incubated. Cells were washed with media prior to addition of nanoparticle−protein conjugates suspended in 1 mL of fresh media.

**Procedure for Staining the Cells.** The position and integrity of the internalized nanoparticle−protein conjugates were evaluated by confocal microscopy. For these experiments, we have stained the nucleus and lysosomal compartments of the cell and used fluorescent nanoparticle−protein conjugates. All of the stains were added to the cell media and mixed properly. Lysotracker red ($\lambda_{ex}$ = 577 nm, $\lambda_{em}$ = 590 nm, 0.5 mM) was added to the cell sample 2 h prior to imaging.

Cell nuclei were stained using DAPI (dilactate) by adding 10 μL of DAPI ($\lambda_{ex}$ = 405 nm, $\lambda_{em}$ = 460 nm, 0.1 μM) with proper mixing and incubated for 10 min. For tracking the nanoparticle−protein conjugates, dye-doped silica nanoparticles containing Rubpy ($\lambda_{ex}$ = 458 nm, $\lambda_{em}$ = 592 nm) conjugated with green fluorescent protein (GFP) ($\lambda_{ex}$ = 488 nm, $\lambda_{em}$ = 515 nm) were added to cells. Stained samples were washed thoroughly with 1 mL of fresh DMEM at least three times and imaged. All stains were purchased from Invitrogen, USA. Confocal microscopy images were obtained and processed using LSM Image Browser. To distinguish between lysotracker and Rubpy (which have close $\lambda_{em}$ values), we have rendered Rubpy using a yellow palette.

**Fluorescence Assisted Cell Sorting (FACS).** Cells were seeded in a 12-well plate at a density of 3 × $10^5$ cells/well and incubated for 4−6 h. The cells were then washed with DMEM and incubated with a solution of nanoparticle−protein conjugates diluted in fresh media for various time periods (1−14 h). For FACS analysis, cells incubated with nanoparticle−protein conjugates were washed with fresh DMEM, PBS, and then detached from the surface by incubating with 300 μL of 0.05% trypsin/EDTA mixture. Samples collected were resuspended in DMEM. Nanoparticle−protein conjugates not internalized into the cells were removed from the cell suspension by centrifuging the cells at 1000 rpm for 3 min and resuspending cells in fresh DMEM. The resulting cell suspension was diluted in an equal volume of FACS Flow (BD Biosciences) followed by analysis on FACS.

The cell suspensions were analyzed on a BD Sciences LSRII flow cytometer. The forward scatter (FSC) and side scatter (SSC) for the cells were adjusted using MCF-7 cells (control) to lie in a range of 50−100 and were appropriately gated to include the majority of live cell population. FITC-A signal ($\lambda_{ex}$ = 488 nm, $\lambda_{em}$ = 515 nm) for cells without any fluorophore was adjusted to obtain a background signal of *ca.* 2000 for control cells. Cells suspensions with nanoparticle conjugates were analyzed with the same settings, and at least 5000 events were obtained for each sample in the gate selected for control cells. Data were analyzed and plotted using Flow Jo software.

**Protein Transfection Using Pro-Ject.** Cells were seeded in a 12-well plate at a density of 3 × $10^5$ cells/well and incubated for 4−6 h. GFP (in 50 μL) was added to a microcentrifuge tube containing the dry film of Pro-Ject reagent (prepared using the standard protocol supplied by the provider) and incubated for 5 min. The

Pro-Ject protein complexes were mixed with 450 μL of serum-free DMEM and added to cells in the 12-well plate and incubated for 4 h. At the end of incubation, the medium in the well was changed to fresh DMEM containing 5% FBS. Transfected cells were characterized by FACS as described above.

**Toxicity Assay.** Cells were seeded in a 12-well plate at a density of $3 \times 10^5$ cells/well and incubated for 4−6 h. Cells were then washed with DMEM and incubated overnight with a solution of nanoparticle−protein conjugates diluted in fresh media. Cell media from each sample were collected, and cells were detached by incubating with 300 μL of 0.05% trypsin/EDTA mixture. Detached cells were then suspended in the media previously collected from the sample. Cell suspension was diluted with Trypan Blue reagent in a 1:1 ratio, and live and dead cells were counted on a hemacytometer.

**Western Blot.** Cells were seeded in a 12-well plate at a density of $3 \times 10^5$ cells/well and incubated for 4−6 h. SiNP−anti-pAkt conjugates were prepared by adding 50 μL (5 μg of anti-pAkt mAb with 5 μg BSA, Phospho-Akt (Ser473) mAb #4058, Cell Technology, Inc. MA). of the anti-pAkt mAb solution to 4 mg of SiNP conjugates. Cells were washed with DMEM, and a solution of SiNP−pAkt antibody conjugates diluted in fresh media was then added to the wells and incubated overnight. At the end of incubation, cells were washed with PBS and lysed. The solutions containing cell lysates were heated at 95 °C for 15 min followed by characterization by SDS-PAGE on a 10% SDS gel at 120 V. The protein bands were transferred to a PVDF membrane. PARP cleavage was observed using anti-PARP rabbit mAB (#9542, Cell Technology, Inc. MA). as the primary antibody, and goat antirabbit IgG, HRP-linked antibody as the secondary antibody.

*Acknowledgment.* We acknowledge the financial support from the Nanoscale Science and Engineering Initiative of the National Science Foundation under NSF Award Number DMR-0642573. We thank Prof. David Schaffer for providing the rat NSCs.

*Supporting Information Available:* Additional data supporting the results, including movies, orthogonal projections, and toxicity assays. This material is available free of charge *via* the Internet at http://pubs.acs.org.

## REFERENCES AND NOTES

1. Schwarze, S. R.; Dowdy, S. F. *In Vivo* Protein Transduction: Intracellular Delivery of Biologically Active Proteins, Compounds and DNA. *Trends Pharmacol. Sci.* **2000**, *21*, 45–48.
2. Ford, K. G.; Souberbiele, B. E.; Darling, D.; Farzaneh, F. Protein Transduction: An Alternative to Genetic Intervention. *Gene Ther.* **2001**, *8*, 1–4.
3. Paddison, P. J. RNA Interference in Mammalian Cell Systems. In *RNA Interference: Current Topics in Microbiology and Immunology*; Springer: Berlin, 2008; Vol. 320, pp 1−19.
4. Vivanco, I.; Sawyers, C. L. The Phosphatidylinositol 3-Kinase-AKT Pathway in Human Cancer. *Nat. Rev. Cancer* **2002**, *2*, 489–501.
5. Chang, H. RNAi-Mediated Knockdown of Target Genes: A Promising Strategy for Pancreatic Cancer Research. *Cancer Gene Ther.* **2007**, *14*, 677–685.
6. Leader, B.; Baca, Q. J.; Golan, D. E. Protein Therapeutics: A Summary and Pharmacological Classification. *Nat. Rev. Drug Discovery* **2008**, *7*, 21–39.
7. Lee, K. D.; Oh, Y. K.; Portnoy, D. A.; Swanson, J. A. Delivery of Macromolecules into Cytosol Using Liposomes Containing Hemolysin from Listeria Monocytogenes. *J. Biol. Chem.* **1996**, *271*, 7249–7252.
8. Provoda, C. J.; Stier, E. M.; Lee, K. D. Tumor Cell Killing Enabled by Listeriolysin *O*-Liposome-Mediated Delivery of the Protein Toxin Gelonin. *J. Biol. Chem.* **2003**, *278*, 35102–35108.
9. Futami, J.; Kitazoe, M.; Maeda, T.; Nukui, E.; Sakaguchi, M.; Kosaka, J.; Miyazaki, M.; Kosaka, M.; Tada, H.; Seno, M.; *et al.* Intracellular Delivery of Proteins into Mammalian Living Cells by Polyethylenimine-Cationization. *J. Biosci. Bioeng.* **2005**, *99*, 95–103.
10. Slowing, I. I.; Trewyn, B. G.; Lin, V. S. Y. Mesoporous Silica Nanoparticles for Intracellular Delivery of Membrane-Impermeable Proteins. *J. Am. Chem. Soc.* **2007**, *129*, 8845–8849.
11. Kam, N. W. S.; Jessop, T. C.; Wender, P. A.; Dai, H. J. Nanotube Molecular Transporters: Internalization of Carbon Nanotube−Protein Conjugates into Mammalian Cells. *J. Am. Chem. Soc.* **2004**, *126*, 6850–6851.
12. Jiang, W.; Kim, B. Y. S.; Rutka, J. T.; Chan, W. C. W. Nanoparticle-Mediated Cellular Response Is Size-Dependent. *Nat. Nanotechnol.* **2008**, *3*, 145–150.
13. Kostarelos, K.; Lacerda, L.; Pastorin, G.; Wu, W.; Wieckowski, S.; Luangsivilay, J.; Godefroy, S.; Pantarotto, D.; Briand, J. P.; Muller, S.; *et al.* Cellular Uptake of Functionalized Carbon Nanotubes Is Independent of Functional Group and Cell Type. *Nat. Nanotechnol.* **2007**, *2*, 108–113.
14. Torchilin, V. P. Recent Approaches to Intracellular Delivery of Drugs and DNA and Organelle Targeting. *Annu. Rev. Biomed. Eng.* **2006**, *8*, 343–375.
15. Wang, H. M.; Yu, S. W.; Koh, D. W.; Lew, J.; Coombs, C.; Bowers, W.; Federoff, H. J.; Poirier, G. G.; Dawson, T. M.; Dawson, V. L.; *et al.* Apoptosis-Inducing Factor Substitutes for Caspase Executioners in NMDA-Triggered Excitotoxic Neuronal Death. *J. Neurosci.* **2004**, 10963–10973.
16. Andrabi, S.; Kim, N. S.; Yu, S. W.; Wang, H.; Koh, D. W.; Sasaki, M.; Klaus, J. A.; Otsuka, T.; Zhang, Z.; Koehler, R. C.; Hurn, P. D.; Poirier, G. G.; Dawson, V. L.; Dawson, T. M. Poly(ADP-ribose) (PAR) Polymer Is a Death Signal. *Proc. Natl. Acad. Sci. U.S.A.* **2006**, *103*, 18308–18313.
17. Pantarotto, D.; Briand, J. P.; Prato, M.; Bianco, A. Translocation of Bioactive Peptides across Cell Membranes by Carbon Nanotubes. *Chem. Commun.* **2004**, 16–17.
18. Verma, A.; Uzun, O.; Hu, Y. H.; Hu, Y.; Han, H. S.; Watson, N.; Chen, S. L.; Irvine, D. J.; Stellacci, F. Surface-Structure-Regulated Cell-Membrane Penetration by Monolayer-Protected Nanoparticles. *Nat. Mater.* **2008**, *7*, 588–595.
19. Kam, N. W. S.; O'Connell, M.; Wisdom, J. A.; Dai, H. J. Carbon Nanotubes as Multifunctional Biological Transporters and Near-Infrared Agents for Selective Cancer Cell Destruction. *Proc. Natl. Acad. Sci. U.S.A.* **2005**, *102*, 11600–11605.
20. Lu, C. W.; Hung, Y.; Hsiao, J. K.; Yao, M.; Chung, T. H.; Lin, Y. S.; Wu, S. H.; Hsu, S. C.; Liu, H. M.; Mou, C. Y.; Yang, C. S.; Huang, D. M.; Chen, Y. C. Bifunctional Magnetic Silica Nanoparticles for Highly Efficient Human Stem Cell Labeling. *Nano Lett.* **2007**, *7*, 149–154.
21. Kam, N. W. S.; Dai, H. J. Carbon Nanotubes as Intracellular Protein Transporters: Generality and Biological Functionality. *J. Am. Chem. Soc.* **2005**, *127*, 6021–6026.
22. Shimomura, O.; Johnson, F. H.; Saiga, Y. Extraction, Purification and Properties of Aequorin, a Bioluminescent Protein from Luminous Hydromedusan, Aequorea. *J. Cell. Comp. Physiol.* **1962**, *59*, 223.
23. Mayor, S.; Pagano, R. E. Pathways of Clathrin-Independent Endocytosis. *Nat. Rev. Mol. Cell Biol.* **2007**, *8*, 603–612.
24. Torchilin, V. P.; Rammohan, R.; Weissig, V.; Levchenko, T. S. TAT Peptide on the Surface of Liposomes Affords Their Efficient Intracellular Delivery Even at Low Temperature and in the Presence of Metabolic Inhibitors. *Proc. Natl. Acad. Sci. U.S.A.* **2001**, *98*, 8786–8791.
25. Kim, J. S.; Yoon, T. J.; Yu, K. N.; Noh, M. S.; Woo, M.; Kim, B. G.; Lee, K. H.; Sohn, B. H.; Park, S. B.; Lee, J. K.; Cho, M. H. Cellular Uptake of Magnetic Nanoparticle Is Mediated through Energy-Dependent Endocytosis in A549 Cells. *J. Vet. Sci.* **2006**, *7*, 321–326.
26. Schein, C. H. From Housekeeper to Microsurgeon: The Diagnostic and Therapeutic Potential of Ribonucleases. *Nat. Biotechnol.* **1997**, *15*, 529–536.
27. Oliver, F. J.; de la Rubia, G.; Rolli, V.; Ruiz-Ruiz, M. C.; de Murcia, G.; Menissier-de Murcia, J. Importance of Poly(ADP-ribose) Polymerase and Its Cleavage in Apoptosis—Lesson from an Uncleavable Mutant. *J. Biol. Chem.* **1998**, *273*, 33533–33539.

28. Oliver, F. J.; Menissier-de Murcia, J.; de Murcia, G. Poly(ADP-ribose) Polymerase in the Cellular Response to DNA Damage, Apoptosis, and Disease. *Am. J. Hum. Genet.* **1999**, *64*, 1282–1288.
29. Reya, T.; Morrison, S. J.; Clarke, M. F.; Weissman, I. L. Stem Cells, Cancer, and Cancer Stem Cells. *Nature.* **2001**, *414*, 105–111.
30. Smith, A. G. Embryo-Derived Stem Cells: Of Mice and Men. *Annu. Rev. Cell Dev. Biol.* **2001**, *17*, 435–462.
31. Schugar, R. C.; Robbins, P. D.; Deasy, B. M. Small Molecules in Stem Cell Self-Renewal and Differentiation. *Gene Ther.* **2008**, *15*, 126–135.
32. Lai, K.; Kaspar, B. K.; Gage, F. H.; Schaffer, D. V. Sonic Hedgehog Regulates Adult Neural Progenitor Proliferation *In Vitro* and *In Vivo*. *Nat. Neurosci.* **2003**, *6*, 21–27.